Thermochimica Acta, 53 (1982) 29–37
Elsevier Scientific Publishing Company, Amsterdam—Printed in The Netherlands

THERMOGENESIS: RELATIVE KINETIC LIMITS

E. CESARI, J ORTIN, V TORRA and J VIÑALS

Departament de Termologia, Facultat de Fisica, Diagonal 645, Barcelona 28 (Spain)

J.L MACQUERON

Laboratoire de Traitement de Signal et Ultrasons, INSA, 69621 Villeurbanne (France)

J P DUBES and H TACHOIRE

Laboratoire de Thermochimie, Universite de Provence, 13331 Marseille Cedex 3 (France)

(Received 30 July 1981)

ABSTRACT

This work presents kinetic limits for conduction calorimeters taken from experimental data and given in reduced units ($\nu\tau_1$) Two different criteria are proposed concerning either a full reconstruction of a rectangular heat pulse (used in calibration procedures) or a complete separation of elementary pulses to provide a fair reconstruction of the thermogenesis These upper limits are given for several signal to noise ratios

INTRODUCTION

The study carried out recently on conduction calorimeters has focussed on a numeric and electronic approach to thermogenesis, presenting, for instance, comparative results given by inverse filters [1,2], analytic approximations to the transfer function (TF) of the system [3–5] and harmonic analysis. Calorimetric models have allowed an analysis of the effects introduced by the existence of experimental noise and the consideration of an upper frequential limit in the deconvolutive calculus [5,6].

The kinetic possibilities of a calorimetric device depend on the frequential characteristics of the response to a Dirac pulse, on the spectrum of the signal which is to be deconvoluted and, finally, on the signal to noise ratio.

Taking for granted a relative scale representation both in time and frequency, this work puts forward quantitative criteria to reconstruct fairly an arbitrary thermogenesis. These criteria allow an estimate of the kinetic possibilities of several conduction calorimeters in terms of their first time constant.

0040-6031/82/0000–0000/$02 75

IDENTIFYING THE PATTERN OF THE THERMOGENESIS

Once the linearity of the calorimetric device has been well established we may take into account the superposition principle: the feasibility of reconstructing an arbitrary thermogenesis—sampled with a period T—depends on the performance of the calorimeter in reconstructing rectangular heat dissipations (Fig. 1A).

The spectrum of a rectangular pulse is represented by its Fourier integral. If we have a sequence of pulses, it is easily represented by a Fourier series (Figs. 1B and 1C). The Fourier transformation of a rectangular pulse of height W and width T is

$$\hat{f}(\omega) = \frac{1}{\sqrt{2\pi}} \frac{W}{\omega} \{\sin(\omega T) + i(\cos(\omega T) - 1)\}$$

The Fourier series for the sequence of pulses is

$$f(t) = W\left\{\frac{1}{2} + \frac{2}{\pi}\left[\sin\frac{2\pi t}{2T} + \frac{1}{3}\sin 3\frac{2\pi t}{2T} + \frac{1}{5}\sin 5\frac{2\pi t}{2T} + \ldots\right]\right\}$$

whose characteristic frequencies are (see arrows in Fig. 1C)

$\nu_0 = 1/2T;\ 3/2T;\ 5/2T;\ldots;\ (2n+1)/2T$

The quality of the resultant thermogenesis depends on the amplitude of the spectrum considered in the deconvolution. A finite inverse transform yields a periodic ripple superimposed on the thermogenesis that can be suppressed using an adequate averaging technique [5]. Figure 2A makes evident that in order to obtain a fair thermogenesis we must consider a high enough cut-off frequency ν_c ($\nu_c = A\nu_0, \nu_0 = 1/2T$). Figure 2C presents the reconstruction corresponding to $A \simeq 9$. With this choice of the cut-off frequency the uprise from 10% to 90% of the total height of the pulse takes place in less than $T/10$.

However, if one only needs a complete separation of the pulses and their intensity (Fig. 2B), it is enough to consider a cut-off frequency $\nu_c > 3\nu_0$.

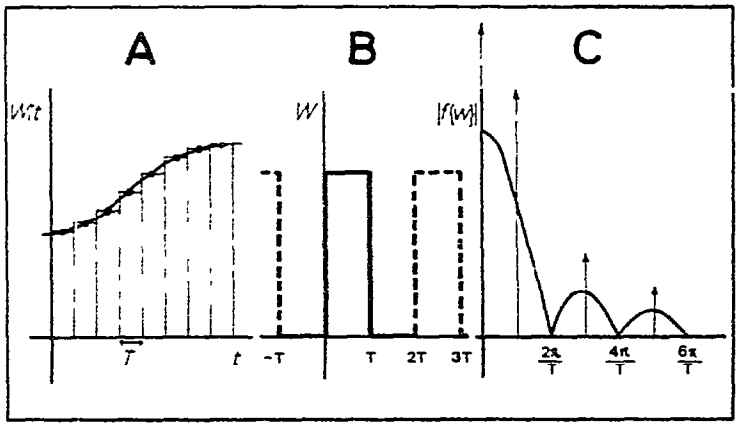

Fig 1 A) Decomposition of an arbitrary heat power dissipation $W(t)$ in elementary rectangles. The sampling period is T B) Rectangular pulse or width T (solid line) and sequence of pulses (dashed line) C) Modulus of the Fourier integral of the pulse The arrows represent the frequencies which appear in the Fourier series of the sequence of pulses

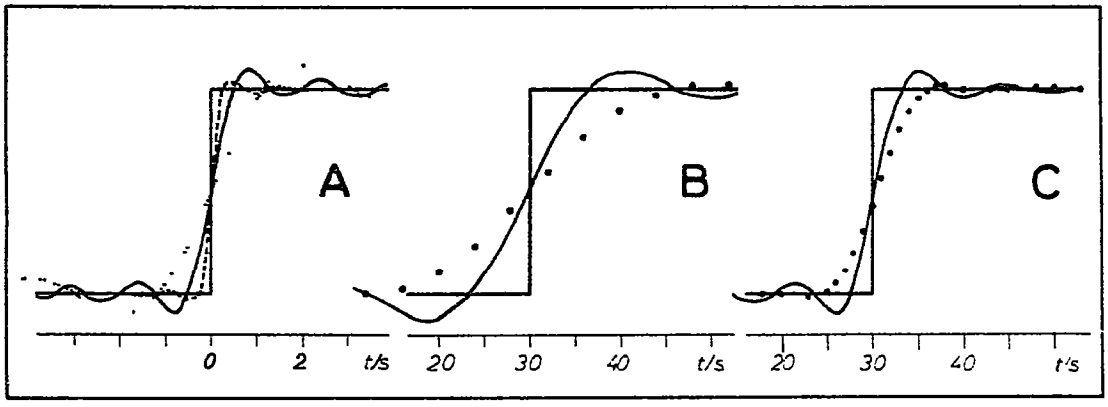

Fig 2 A) Reconstruction of a pulse of $T=8$ s considering successive terms of its Fourier series · , 3 terms, (————), 6 terms; - - - - -, 41 terms B) Reconstruction of a pulse of $T=40$ s ($\nu_0=0\,013$ Hz) by means of the FFT The solid line represents a finite inverse transform with $\nu_c=0\,042$ Hz $\simeq 3\nu_0$ Averaging this curve gives that represented by a dotted line C) Reconstruction of the same pulse with $\nu_c=0\,112$ Hz $\simeq 9\nu_0$ Again the dotted curve is averaged

PRACTICAL CUT-OFF FREQUENCIES

The thermogenesis, within the context of the harmonic analysis, is obtained by means of the Fast Fourier Transform (FFT). This routine handles N points in such a way that $N=2^M$. This fact limits the number of data used depending on the available computer.

In our case, we have $M=10,\ 11,\ 12$ ($N=1024, 2048, 4096$). There is an upper bound for the frequency to be used in the deconvolutive calculus, ν_{Sh}, Shannon frequency, related to the sampling period: $\nu_{Sh}=1/\Delta t$. Frequencies are discrete. $\Delta\nu=\nu_{Sh}/N$ and, consequently, the choice of the cut-off frequency is not arbitrary especially when a simple suppression of the ripple is intended. Figure 3 shows two easy averaging possibilities to suppress the ripple through the expression

$$x'(t_i)=\left(kx(t_i)+\sum_{\substack{j=i-L\\ j\neq i}}^{i+L}x(t_j)\right)/(k+2L)$$

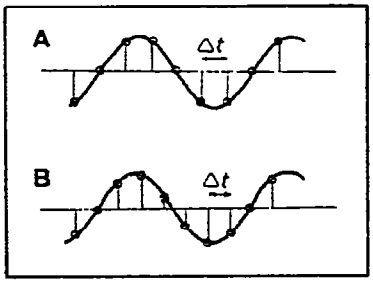

Fig. 3. Two averaging possibilities whether the period of the ripple is a multiple of 2 or not. (A) shows a period of $6\Delta t$ and correspondingly $k=2$. Conversely, (B) corresponds to a period $7\Delta t$ where $k=1$.

TABLE I

N is the number of points handled by the FFT routine; $(N_c - 1)\Delta\nu$ is the cut-off frequency, where N_c can be obtained using $N_c = N/n + 1$ where n is an integer. $(k + 2L)\Delta t$ is the period of the ripple and an (*) means that $k = 1$, otherwise $k = 2$

N											
1024	N_c	513	342	257	206	172	147	129	115	103	94
	L	1	1*	2	2*	3	3*	4	4*	5	5*
2048	N_c	1025	684	513	411	342	294	257	229	206	187
	L	1	1*	2	2*	3	3*	4	4*	5	5*
4096	N_c	2049	1366	1025	820	684	586	513	456	411	373
	L	1	1*	2	2*	3	3*	4	4*	5	5*

with $L = 3$ and $k = 2$ in Fig. 3A and $L = 3$ and $k = 1$ in Fig. 3B.

Now the deconvolution may be carried out easily by means of the FFT. The symmetry of the spectrum around $N/2 + 1$ allows

$$\mathrm{Re}[\hat{f}'(\omega_i)] = 2\mathrm{Re}[\hat{f}(\omega_i)]$$

$$\mathrm{Im}[\hat{f}'(\omega_i)] = 2\mathrm{Im}[\hat{f}(\omega_i)] \qquad 1 < i < N/2 + 1$$

and to annull $\mathrm{Re}[\hat{f}'(\omega_i)]$, $\mathrm{Im}[\hat{f}'(\omega_i)]$ for $i > N_c$. N_c corresponds to the cut-off frequency selected $\nu_c = (N_c - 1)\Delta\nu$. Table I presents several cut-off frequencies which eliminate simply the aforementioned ripple.

RESULTS

1. To ascertain the kinetic possibilities of actual calorimetric systems we have studied different calorimeters represented by their TF plotted versus a relative frequency scale ($\nu\tau_1$) up to the limit imposed by the ratio signal/noise. Figure 4 clearly shows that the frequency range attainable by any conduction calorimeter is not actually much larger than that of the calorimeter JLM-E1. We have focussed our analysis upon the TF of this calorimeter considering, though, two different heat dissipations: either near to the axis of the cellule (measurement L88) or near to the detector system (measurement L89). The TF's have been obtained from thermogenesis whose maximum ordinates are 170926 nV (L88) and 184754 nV (L89). Noise ranges around ± 5 nV (in both cases). (signal/noise $\cong$ 85 dB). Then we have

$\nu_n \simeq 0.08$ Hz (axial) $\quad \nu_n \simeq 0.33$ Hz (co-axial)

or in reduced units:

$\nu_n\tau_1 \simeq 16$ (axial) $\quad \nu_n\tau_1 \simeq 64$ (co-axial)

2. We have used rectangular heat dissipations of 2, 4, 8, 16, 32, 64 s (Fig. 5) to

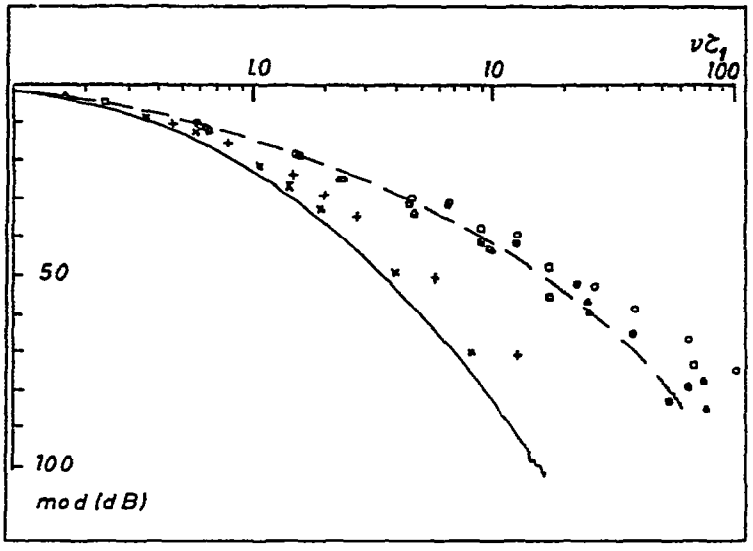

Fig 4 Modulus (dB) vs a reduced frequency scale ($\nu\tau_1$) of several calorimeters ————, — — —, calorimeter JLM-E1 containing silicone oil (see Fig 1, ref 5), ●, ○, large capacity Tian-Calvet calorimeters containing Hg (see Table 1, ref 4) corresponding to different locations of the sources, ▩, □, calorimeter Tib containing Hg (Table 1, ref 3); ▲, △, Tian-Calvet calorimeter, cell volume 15 cm^3 and contains Hg (Table 1, ref 3), +, ×, Tian-Calvet calorimeter, 15 cm^3 with H_2O and sulphur respectively (Table 1, ref 3)

determine the kinetic limits of the calorimeter (Table 2). This table also includes those frequencies which allow a fair reconstruction of the thermogenesis. The deconvolution of the thermogram is presented in Figs. 6 (axial dissipation) and 7 (co-axial or near the detectors). The cut-off frequencies selected are $171\Delta\nu = 0.083$ Hz ($\nu\tau_1 = 16$) and $683\Delta\nu = 0.333$ Hz ($\nu\tau_1 = 64$), respectively. Both frequencies are related within a factor 4 which means that a deconvolutive calculus considering pulses of width T and $T/4$ would be equivalent (see, for instance, Fig. 6B and B′ and Fig. 7A and A′). According to the identification criterium we are able to separate pulses whose period is, at least, $\gtrsim 8$ s (axial) and $\gtrsim 2$ s (co-axial) (see again Fig. 6B and B′ and Fig. 7A and A′). On the other hand the reconstruction criterium yields: $\gtrsim 32$ s (axial) and $\gtrsim 8$ s (co-axial) (see Fig. 6C and C′ and Fig. 7B and B′). Figures 6A and A′ correspond to cut-off frequencies less than $3\nu_0$ and the deconvolution fails to separate different pulses. Conversely, Figs. 7C and C′ correspond to a ν_c greater than $9\nu_0$.

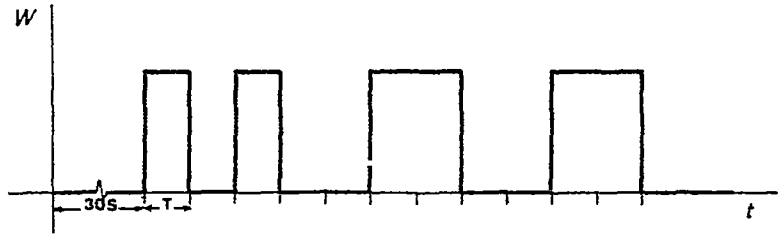

Fig 5. Sequence of pulses defined in Table 2

TABLE 2

Experimental data corresponding to Figs 6 and 7. Cut-off frequencies required to reconstruct or separate pulses of width T

Measurement (axial)	L91	L91	L96	L96	A3	A3
Heat power (mW)	63 25	63 25	15 76	15 76	3 956	3 956
Measurement (co-axial)	L97	L97	L99	L99	A4	A4
Heat power (mW)	39 31	39.31	10 08	10 08	5 696	5 696
Pulse's width, T(s)	2	4	8	16	32	64
$\nu_0 = 1/2T$	0 250	0 125	0 062	0 031	0 016	0 008
Separation						
$3\nu_0$ (Hz)	0 75	0 375	0 188	0 094	0 047	0 023
$3\nu_0\tau_1$	144	72	36	18	9	4 5
Reconstruction						
$9\nu_0$ (Hz)	2 25	1 125	0 563	0 281	0 141	0 070
$9\nu_0\tau_1$	432	216	108	54	27	13 5

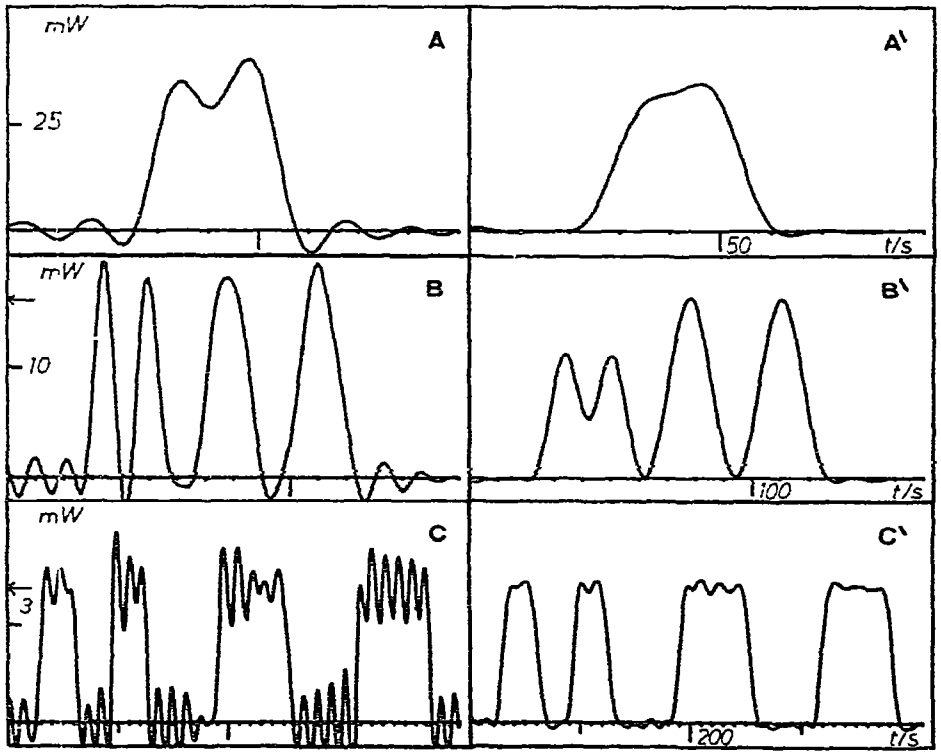

Fig 6 Deconvolution by means of the FFT of a sequence of pulses generated in an axial resistance in the calorimetric vessel, measurements L91 (A and A'), L96 (B and B') and A3 (C and C') $N_c = 172$ in all cases and the primed letters mean that the thermogenesis has been already averaged The arrows indicate the power actually dissipated

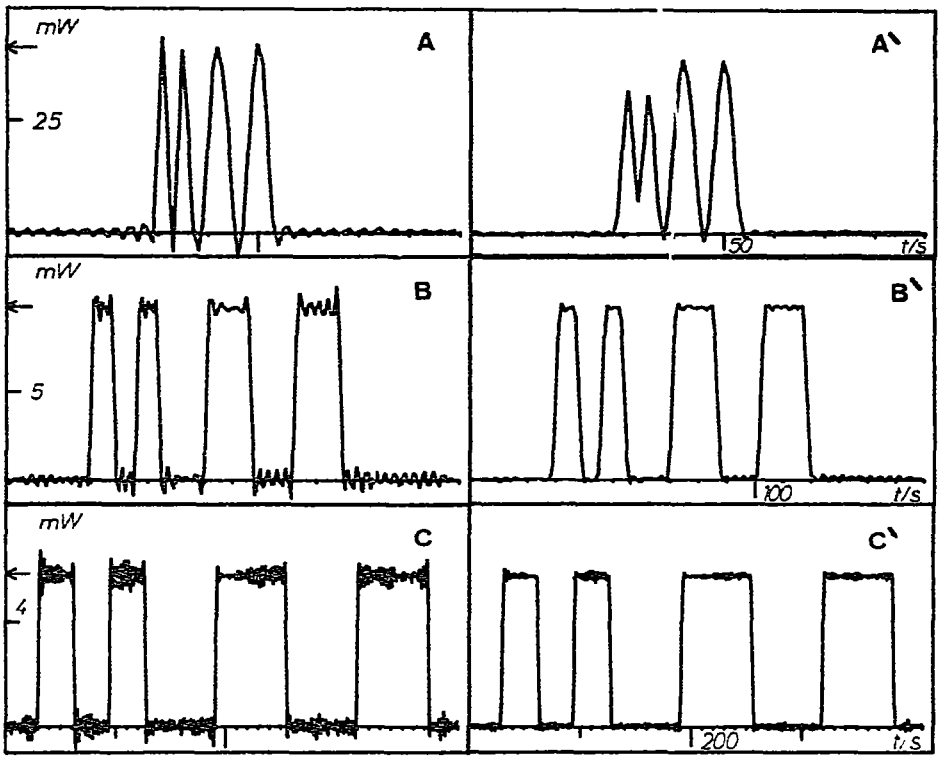

Fig 7 Deconvolution by means of the FFT of a sequence of pulses generated in a co-axial resistance placed near the detector system, measurements L97 (A and A'), L99 (B and B') and A4 (C and C') $N_c = 684$ in all cases and the primed letters stand for the same thermogenesis after having been averaged

KINETIC LIMITS

Inspection of Fig. 4 makes it evident that depending on the ratio signal/noise there are limits on the attainable frequencies once the location of the heat dissipation is given (Table 3).

From these frequencies we have obtained $\overline{\nu\tau_1} = \sqrt{(\nu\tau_1)_{int}(\nu\tau_1)_{ext}}$ and f. Roughly $(\nu\tau_1)_{int} \simeq \overline{\nu\tau_1}/f$ and $(\nu\tau_1)_{ext} \simeq \overline{\nu\tau_1} \cdot f$ (Table 3).

TABLE 3

Relative kinetic limits ($\nu\tau_1$) (taken from experimental data, Fig 4) for signal/noise ratios ranging from 40 to 100 dB and the widths (in a relative time scale) of the rectangular pulses which can be either reconstructed or separated once the frequential limits are known (*, extrapolated)

	$\nu\tau_1$ (axial)	$\nu\tau_1$ (co-axial)	$\overline{\nu\tau_1}$	f	$(\overline{T}/\tau_1)$ reconstruct	$(\overline{T}/\tau_1)$ separate
40 dB	2 5	10	5	2	0.90	0 30
60 dB	5 5	30	13	2 3	0 35	0 12
80 dB	10	60	24	2 4	0.19	0 06
100 dB	20	100*	45	2 2	0 10	0 03

$\overline{\nu\tau_1}$ yields information about the kinetic possibilities according to different signal/noise ratios. This value applies to all calorimeters being independent of the position of the source and the material contained in the laboratory cell (good or poor conductor). When a good conductor is involved, the dispersion in the TF's corresponding to different locations of the dissipation diminishes considerably and the values of $\overline{\nu\tau_1}$ group around $(\nu\tau_1)_{ext}$ ($f \simeq 1$).

The different performances in reconstructing rectangular pulses, in terms of $\overline{\nu\tau_1}$, are summarized in Table 3, either in obtaining a fair reproduction of the pulse or being simply able to separate different signals and to obtain the power dissipated.

REMARK

The remaining ripple after having averaged the thermogenesis is due to: a) signal/noise ratio being lower in an actual thermogenesis ($\approx 10\%$) than that of the TF for sequences of width greater than 8 s; b) (unimportant in this case) the thermogram noise which produces a 0.2 μW noise on the thermogenesis.

CONCLUSIONS

1. The reconstruction of the pattern of a rectangular pulse of width T/τ_1 requires a relative frequency range in the deconvolutive calculus extending beyond $\overline{\nu\tau_1} > 9\tau_1/2T$.

2. A full separation of pulses separated by T/τ_1 needs frequencies higher than $\overline{\nu\tau_1} > 3\tau_1/2T$. "Separation" includes the value of the power dissipated. One needs to consider relative frequencies for the criterium only ensures the obtaining of correct points of the thermogenesis separated by T/τ_1, so defining a new sampling period for the final result even though the sampling period was $\Delta t (\Delta t \sim \tau_1/300)$.

3. The kinetic possibilities of a conduction calorimeter, within a large domain of cell contents and effective cell volumes, depend on the ratio signal/noise. The average upper bounds are $\overline{\nu\tau_1}(40\ \text{dB}) \simeq 5$, $f(40\ \text{dB}) \simeq 2$; $\overline{\nu\tau_1}(60\ \text{dB}) \simeq 13$, $f(60\ \text{dB}) \simeq 2.3$; $\overline{\nu\tau_1}(80\ \text{dB}) \simeq 24$, $f(80\ \text{dB}) \simeq 2.4$. The extreme values (taking into account the different locations of the sources) may be obtained from $(\nu\tau_1)_{max} = \overline{\nu\tau_1} \cdot f$; $(\nu\tau_1)_{min} = \overline{\nu\tau_1}/f$.

ACKNOWLEDGEMENTS

We thank the Service Scientifique of the French Embassy in Spain for their financial aid in the contacts held by the three groups. V.T. gratefully acknowledges aid from C.I.E.S. (France) for a scientific stay at French laboratories and J.O. acknowledges a studentship from the I.N.A.P.E. (Spain).

REFERENCES

1 E Cesari, V Torra, J L Macqueron, R Prost, J P Dubes and H Tachoire, Thermochim Acta, 53 (1982) 17.
2 E Cesari, V Torra, J L Macqueron, R Prost, J P Dubes and H Tachoire, Thermochim Acta, 53 (1982) 1
3 E Cesari, J Ortin, V Torra, J Viñals, J L Macqueron J P Dubes and H Tachoire, Thermochim Acta, 40 (1980) 269
4 E Cesari, J. Ortin, V. Torra, J Viñals, J L Macqueron, J P Dubes and H Tachoire, Thermochim Acta, 43 (1981) 305
5 E Cesari, J Ortin, P Pascual, V Torra, J Viñals, J L Macqueron, J P Dubes and H Tachoire, Thermochim Acta, 48 (1981) 367
6 E Cesari, J Ortin, V Torra, J Viñals, E Utzig and W Zielenkiewicz, An Fis , in press